CO_2 Solubility Modelling in Non-Precipitating Aqueous Solutions of Potassium Lysinate

Antonio Conversano[a,b], Serena Delgado[c,d], Christophe Coquelet[c,e*], Stefano Consonni[a,b], Manuele Gatti[a]

a Dipartimento di Energia, Politecnico di Milano, via Lambruschini 4, 20156 Milano, Italia

b LEAP-Laboratorio Energia ed Ambiente Piacenza, via Nino Bixio 27/C, 29121 Piacenza, Italia

c Mines ParisTech, PSL University, Centre of Thermodynamics of Processes (CTP), 35, rue Saint Honoré, 77305 Fontainebleau cedex, France

d TotalEnergies Tour Coupole, La Défense, 2 Pl. de la Coupole-Jean Millier, 92400

e Université de Toulouse, Mines Albi, Centre RAPSODEE UMR CNRS 5302, Campus Jarlard, Albi, France

*corresponding author: christophe.coquelet@mines-paristech.fr

ABSTRACT

Modelling of CO_2 solubility in aqueous solutions of potassium lysinate (LysK) is mainly hindered by scarcity of experimental vapor-liquid equilibrium data and lack of chemical equilibrium constants associated to the reaction mechanism for the CO_2/LysK/H_2O system. Therefore, Kent-Eisenberg (KE) correlation stands out from the literature, being among the most used approaches for the description of the equilibrium CO_2 partial pressure at different loadings. In this work, a Kent-Eisenberg-like approach has been developed, enhancing the empirical Kent-Eisenberg with Debye-Hückel activity coefficients in order to guide model calibration with reference to selected experimental data for CO_2 solubility in 33.1 and 33.5%$_{w/w}$ aqueous LysK solution; moreover, the KE edition provides an estimation of the missing equilibrium constants. This information has been embedded in a first thermodynamically sound and predictive Deshmukh-Mather (DM) model (average absolute deviation equal to 7%) validated against additional experimental data in a wide temperature and concentration range.

1. Introduction

Global economy expansion in 2018 has been associated with a contextual increase in energy demand, recording 2.3% incremental consumption with respect to 2017. As a result, energy-related CO_2 emissions reached a historic high of 33.1 $GtCO_2$ in the same reference year, with 30% of emissions due to coal fire power generation being the single largest emitter[1]. Overall, the power sector accounted for nearly two-thirds of emissions growth. With reference to 2017, 2018 has seen an estimated 4.6% natural gas consumption increase because of the rise in energy requirement and as a consequence of the progressive coal-to-gas switch, which has contributed for almost 60 Mt of avoided coal and consequent saving of 95 $MtCO_2/y_{2018}$.

To meet the goals of the Paris agreement aiming at an increase in global average temperature "well below" 2°C above pre-industrial levels, the clean energy transition will need to bring about a rapid reduction of greenhouse gases down to net zero CO_2 emissions by the second half of the century. To this end, no single path can be identified. However, the strategic portfolio recommended by researchers and intergovernmental organizations quantifies the role of Carbon Capture, Utilization and Storage (CCUS) technologies to 15% CO_2 of emission savings in 2070[2].

Among the capture technologies, Post Combustion Capture (PCC) is a mature and retrofittable option for CO_2 capture from flue gas for power industry decarbonization. In case of low CO_2 partial pressure in the treated gas stream, PCC-scrubbing with solvents involves CO_2–sorbent chemical reaction, which forms weakly bonded intermediate compounds to be regenerated. This step restores the solvent and releases an isolated CO_2-rich stream ready for dehydration, compression, and storage. PCC-chemical scrubbing has high removal rate and selectivity[3]. Specifically, aqueous monoethanolamine (MEA) at 30%$_{w/w}$ has been taken as a benchmark in several European initiatives focusing on Natural Gas Combined Cycle (NGCC)-flue gas decarbonisation (e.g. projects[4,5]). However, MEA scrubbing shows many drawbacks; among these, high-energy consumption for regeneration, limited CO_2 loading capacity, equipment corrosion and elevated packed volumes of the absorption unit, generation of toxic compounds and amine volatility constitute areas of improvement.

Therefore, new studies on alternative solvents focus on identifying more effective, energy saving and greener solvents for a low-carbon energy production industry. With these regards, amino acid salts (AAS) solutions are attracting the attention of the scientific community working on CO_2 capture[6]: they present the same functional amino group as alkanolamines, they can reach high CO_2 loading capacity and fast reaction rates; moreover, they are considered environmentally friendly, showing low volatility and ecotoxicity, stability against oxidation, together with negligible corrosion effects[7,8].

Research activities on amino acid salts solutions for CO_2 absorption are already ongoing. An important work has been carried out by Siemens Company, which has proposed a carbon capture process known as "POSTCAP", tested at pilot scale[9] and modelled to predict the specific thermal energy demand for solvent regeneration in case of a full-scale capture unit. The POSTCAP technology applied to a coal-fired reference power plant is estimated to require 2.7 MJ/kgCO_2 captured[9] versus a reference value of 3.7 MJ/kgCO_2 for the benchmark solvent (30%$_{w/w}$ MEA solutions).

Literature review, experimental campaigns and data analysis to quantify the absorption potential of selected amino acid salts solutions in NGCC-CO_2 capture applications have been carried out by the authors [10,11]. From this screening, potassium lysinate (LysK) has been identified as a relevant compound due to its high capacity and loading, fast kinetics and significant CO_2 absorption flux. Therefore, further investigation on its potential as a greener option in PCC-scrubbing applications is necessary, requiring vapour-liquid equilibria (VLE) measurements and thermodynamic modelling, CO_2 capture unit design and techno-economic assessment (to quantify e.g., specific reboiler thermal duty required for regeneration, SPECCA index, cost of electricity, cost of CO_2 avoided).

The availability of reliable and accurate information on carbon dioxide equilibrium solubility in aqueous solutions of AAS is of paramount importance to proper design gas treating units. In this area, the literature offers a variety of works mainly based on Kent-Eisenberg (KE) correlation[12–18], with ideal mixture assumption. This framework makes Kent-Eisenberg regressions unfit for extrapolation. Hence, researchers working on CO_2 solubility in aqueous amines have moved towards the application of activity coefficient models such as the electrolyte-NRTL (e-NRTL) model from Chen and Evans[19], and the Deshmukh-Mather model[20], which provide greater rigor and a more thermodynamically-sound methodology.

Although both solutions account for long- and short-range particle interactions, Deshmukh-Mather has demonstrated accuracy and reliability with a computationally affordable price and a simple activity coefficient expression. Kent-Eisenberg is state-of-the-art for the description of the AAS/CO_2/H_2O systems, and is extensively adopted, although very recent publications for different amino acid salts-based systems (e.g., potassium taurate) have applied the e-NRTL model[21] in Aspen® simulator. In the specific case of CO_2 solubility in aqueous potassium lysinate solutions, VLE description still relies on empirical correlations (KE), hence constituting a relevant case-study for more rigorous thermodynamic modelling. Nevertheless, unavailable chemical equilibrium constant parameters are still estimated with KE.

This work is meant to fill the gap, proposing a first semi-empirical thermodynamic model for CO_2 solubility in the non-precipitating LysK/CO_2/H_2O system. The model has been coded in Matlab® using Deshmukh-Mather formulation, while starting from a modified edition of the Kent-Eisenberg correlation (i.e., Kent-Eisenberg endowed with Debye-Hückel activity coefficient expression) used to identify missing carbamate hydrolysis equilibrium constants. The Deshmukh-Mather approach has been selected because of its compact activity coefficient model expression. A comparison against other models with more sophisticated activity coefficient formulations (e.g., e-NRTL) would be beneficial and will be carried out in future works. Moreover, further experimental investigation of vapour-liquid equilibrium of CO_2 in aqueous LysK solution need to be performed to validate the model over a wider loading range compared to the one characterizing the here-identified literature data. Finally, experiments are required for a complete identification of the set of equilibrium constants.

The manuscript is organized as follows: Section 2 defines the thermodynamic problem. It is followed by a description of the used methodology (Section 3) which has allowed the transition from the empirical Kent-

Eisenberg correlation to its formulation which includes activity coefficients; this is sets the ground for the Deshmukh-Mather model definition. Results and discussion are reported in Section 4 while conclusion and perspectives for further the investigation[22] are mentioned in Section 5.

2. Thermodynamic Framework

2.1. Rationale

An appropriate thermodynamic model needs to give an extensive description of CO_2 solubility partial pressure as a function of loading, temperature, and concentration. It should also accurately predict other thermodynamic properties required in energy balance calculations, such as solvent enthalpies, entropies, etc. Models are not completely predictive in nature, and they usually rely on experimental data to provide good correlations. In the literature, it is common to distinguish empirical and semi-empirical (or rigorous) models. The first category includes models consisting in mathematical correlations; they may assume liquid and vapour phase ideal behaviour (which is a strong assumption) with weak or no theoretical background. Common empirical models sometimes lump system non ideality within correction factors or model parameters regressed against experimental data, providing quite reliable yet simple correlations valid within the regression interval of temperature and composition, with consequent accuracy reduction outside of this range. Although modifications could provide accuracy improvements, the intrinsic limitation given by the phase ideality assumption can be detrimental to the validity of this empirical approach, paving the way for rigorous models such as excess Gibbs energy (G^E), equation of state (EoS) and their combination (EoS/G^E). Semi-empirical models are based on the equivalence of single component fugacity in vapour and liquid phase. Sophisticated formulations require the use of equation of state for the gas phase, and an activity coefficient model for the liquid phase, leading to an effective representation of CO_2 solubility in liquid solution for a wide range of operating process parameters because of an increase in model complexity. Nevertheless, rigorous models remain semi-empirical as they adopt calibrated parameters that are tuned against experimental data to guarantee both accuracy in the calibration range and effective prediction outside of it[23].

As previously mentioned, a very common empirical correlation used in the industry to describe CO_2 solubility in amine solutions is the Kent-Eisenberg correlation (discussed in Paragraph 2.3). Kent-Eisenberg approach assumes ideal liquid and gas phases. In previous literature work, the non-ideal behaviour of the system is lumped within the calibrated protonation and carbamate hydrolysis reaction parameters. Therefore, KE assumes that the equilibrium constants are functions of concentration and temperature only, with unitary activity coefficients. The model provides a fair fitting within the calibration interval, but it does not involve any theoretical formulation that justifies extrapolation.

Semi-empirical models rigorously calculate system non-ideality by including activity coefficients within the equilibrium constants. Among the most relevant formulations, Deshmukh and Mather have proposed a model based on the Guggenheim activity coefficient equation, which is a combination of a first term accounting for long-range interactions (electrostatic forces as described by Debye-Hückel) and a second term expressing short range interactions (for more details, Paragraph 2.4).

e-NRTL is an extension of the NRTL model[24] that calculates liquid activity coefficients. This model has been initially proposed for aqueous electrolyte systems[19] but it has been extended for mixed-solvent electrolyte systems. The activity coefficients obtained from this thermodynamic formulation stem from three contributions, namely a Pitzer–Debye–Hückel (PDH) term, a Born term and a NRTL term. PDH is an unsymmetrical normalised contribution proposed by Pitzer[25] for long-range ion-ion interactions existing beyond the immediate neighbourhood of a central ionic species. The Born term is the unsymmetrical normalised contribution[26] accounting for the effect of mixed solvent. It expresses the difference in Gibbs free energy between ionic species in a mixed solvent and in water. The last contribution is the unsymmetrical NRTL normalised contribution related to local interaction in the immediate neighbourhood of any central species. Several examples of e-NRTL model application can be found in the literature: Austgen has represented the vapour-liquid equilibria of acid gas in diethanolamine (DEA) and MEA solutions[27], Borhani

has adopted the model to compare equilibrium and non-equilibrium process models for tray column, also comparing the effect of different amines as promoters on potassium carbonate process[28], Hilliard has completed several thermodynamic models representing CO_2 solubility with amine solvent, dedicating special efforts to aqueous MEA[29].

The extended universal quasi-chemical functional group activity coefficient electrolyte model[30] (e-UNIQUAC) is an additional semi-empirical model that is built upon the UNIQUAC formulation. The e-UNIQUAC excess Gibbs energy expression contains a combinatorial or entropic term accounting for short-range ion-ion interactions. This term only depends on the size of the species, regardless of system temperature. The second residual or enthalpic term for short-range ion-ion interactions is temperature-dependent. Moreover, the additional contribution of the e-UNIQUAC formulation with respect to the UNIQUAC expression is given by a third Debye-Hückel term which accounts for long-range electrostatic interactions. Significant literature adopting e-UNIQUAC model refers to CO_2 solubility description for aqueous MEA solutions carried out by Aronu et al.[31] Other examples include its application for the thermodynamic representation of carbon dioxide absorption in aqueous MEA and methyldiethanolamine (MDEA) solutions by Faramarzi et al.[32].

In case sufficient data are not available, a possible solution for solubility description is the UNIFAC model, which is a group contribution method presented by Fredenslund et al.[33] The model has been used by Ye et al. to predict vapour liquid equilibria and vapour liquid-liquid equilibria for systems constituted by methanol (MeOH), dimethyl ether (DME), CO_2 and H_2O[34]. It predicts the activity coefficients by adding a combinatorial and residual term, averaging group-group interactions of the selected molecules.

In the present application, the rigorous Deshmukh-Mather model has been selected and fully implemented in Matlab® as it provides higher accuracy in terms of solubility description with respect to the empirical Kent-Eisenberg approach and reduced computational effort compared to e.g., e-NRTL[35].

2.2. The thermodynamic problem of the CO_2/LysK/H_2O system

The amino acid salt considered in this work is potassium lysinate (LysK), which has been assessed in the perspective of CO_2 post combustion capture applications via non-precipitating chemical absorption. This choice stems from preliminary results of previous experimental activities at laboratory[36–38] and bench-scale[39]. Solvent selection relies on mass transfer and energy performance indicators. A solvent selection screening methodology has been investigated in previous work[11,39].

From a chemical standpoint, lysine is an organic molecule with one carboxyl group in α position (pKa=2.18 at 25°C), and two amino groups respectively in α (pKa=8.95 at 25°C) and in ε (pKa=10.53 at 25°C) positions[40]. In aqueous solution, Lysine dissociates differently depending on the pH: as represented in Figure 1, the anionic form Lys^- is prevalent at high pH, shifting towards LysH (zwitterionic form) which reaches its highest concentration at the isoelectric point (pI). In acidic solution, $LysH^+$ (cationic form) and $LysH^{2+}$ (di-cationic form) are the prevalent species[41–43].

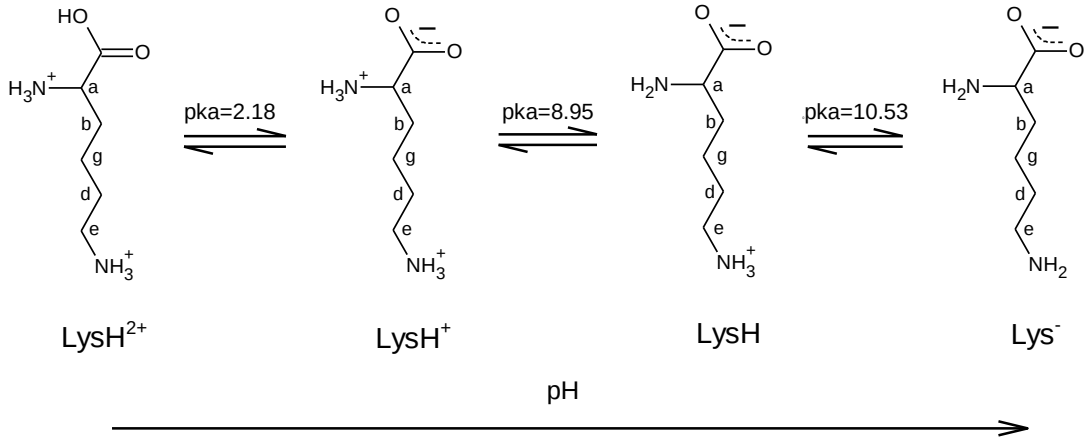

Figure 1: Ionization equilibria of lysine in water-based solutions at 25°C.

Given the presence of amino functional groups, CO_2 is expected to react directly or through an acid-base buffer mechanism with AAS, forming non-volatile ionic species, as with alkanolamines[27,44]

Carbamate hydrolysis reactions:

$$\mathrm{CARB1} + \mathrm{H_2O} \overset{\mathrm{K_{R1}}}{\longleftrightarrow} \mathrm{LysH} + \mathrm{HCO_3^-} \qquad \textit{Eq. 1}$$

$$\mathrm{CARB2} + \mathrm{H_2O} \overset{\mathrm{K_{R2}}}{\longleftrightarrow} \mathrm{Lys^-} + \mathrm{HCO_3^-} \qquad \textit{Eq. 2}$$

Dissociation of protonated amino acid:

$$\mathrm{LysH^+} \overset{\mathrm{K_{LysH^+}}}{\longleftrightarrow} \mathrm{LysH} + \mathrm{H^+} \qquad \textit{Eq. 3}$$

$$\mathrm{LysH} \overset{\mathrm{K_{LysH}}}{\longleftrightarrow} \mathrm{Lys^-} + \mathrm{H^+} \qquad \textit{Eq. 4}$$

Hydrolysis of carbon dioxide:

$$\mathrm{CO_2} + \mathrm{H_2O} \overset{\mathrm{K_{CO_2}}}{\longleftrightarrow} \mathrm{HCO_3^-} + \mathrm{H^+} \qquad \textit{Eq. 5}$$

Dissociation of bicarbonate:

$$\mathrm{HCO_3^-} \overset{\mathrm{K_{HCO_3^-}}}{\longleftrightarrow} \mathrm{CO_3^{2-}} + \mathrm{H^+} \qquad \textit{Eq. 6}$$

Dissociation of water:

$$\mathrm{H_2O} \overset{\mathrm{K_{H_2O}}}{\longleftrightarrow} \mathrm{H^+} + \mathrm{OH^-} \qquad \textit{Eq. 7}$$

Where $CARB1 = NH_3^+ - R_2R_1CH - NHCOO^-$, $CARB2 = {}^-OOCHN - R_2R_1CH{-}NH_2$, $R_1 = -COO^-$ *and* $R_2 = -(CH_2)_4 -$, $LysH = NH_3^+ - R_2R_1CH - NH_2$ and $Lys^- = NH_2 - R_2R_1CH - NH_2$.

Chemical equilibrium is then represented by equilibrium equations (Eq. 8-Eq. 14) considered relevant for the description of CO_2 solubility in aqueous non-precipitating LysK solutions[44]:

$$K_{R1} = \frac{\ddot{a}_{LysH}\ddot{a}_{HCO_3^-}}{\ddot{a}_{CARB1}a_{\mathrm{H_2O}}} \qquad \textit{Eq. 8}$$

$$K_{R2} = \frac{\ddot{a}_{Lys^-}\ddot{a}_{HCO_3^-}}{\ddot{a}_{CARB2}a_{\mathrm{H_2O}}} \qquad \textit{Eq. 9}$$

$$\mathrm{K_{LysH^+}} = \frac{\ddot{a}_{\mathrm{H^+}}\ddot{a}_{\mathrm{LysH}}}{\ddot{a}_{\mathrm{LysH^+}}} \qquad \textit{Eq. 10}$$

$$\mathrm{K_{LysH}} = \frac{\ddot{a}_{\mathrm{H^+}}\ddot{a}_{\mathrm{Lys^-}}}{\ddot{a}_{\mathrm{LysH}}} \qquad \textit{Eq. 11}$$

$$K_{CO_2} = \frac{\ddot{a}_{H^+}\ddot{a}_{HCO_3^-}}{\ddot{a}_{CO_2}a_{H_2O}} \quad \textit{Eq. 12}$$

$$K_{HCO_3^-} = \frac{\ddot{a}_{H^+}\ddot{a}_{CO_3^{2-}}}{\ddot{a}_{HCO_3^-}} \quad \textit{Eq. 13}$$

$$K_{H_2O} = \frac{\ddot{a}_{H^+}\ddot{a}_{OH^-}}{a_{H_2O}} \quad \textit{Eq. 14}$$

Speciation constraints are added to the chemical equilibria equations: amino acid balance, CO_2 balance, total balance and charge balance (Eq. 15-Eq. 18). The system of equations to solve for the liquid-phase speciation consists in Eq. 8-Eq. 18.

$$n_{LysH|_0} = n_{LysH} + n_{LysH^+} + n_{Lys^-} + n_{CARB1} + n_{CARB2} \quad \textit{Eq. 15}$$

$$\alpha n_{LysH|_0} = n_{CO_2} + n_{CARB1} + n_{CARB2} + n_{CO_3^{2-}} + n_{HCO_3^-} \quad \textit{Eq. 16}$$

$$\sum_{i=1}^{C} x_i = 1 \quad \textit{Eq. 17}$$

$$n_{K^+} + n_{H^+} + n_{LysH^+} = n_{Lys^-} + 2n_{CARB2} + n_{CARB1} + 2n_{CO_3^{2-}} + n_{HCO_3^-} + n_{OH^-} \quad \textit{Eq. 18}$$

Where $n_{LysH|_0}$ = $n_{LysK|0}$ is the lysinate apparent mole number in liquid phase and α is the CO_2 loading (molCO_2/mol LysK) and n_i is the mole number of component i. Using a stoichiometric approach, this system of equations has been solved with successive substitutions based on the Newton-Raphson method.

2.3. Kent-Eisenberg Correlation

Kent-Eisenberg model is a widely-used empirical thermodynamic model in the field of acid gas absorption[45] to describe CO_2 vapour-liquid equilibria in aqueous alkanolamine solutions. The chemical reactions equilibrium constants are usually available from the literature, except for carbamation and protonation reactions of amines expressed as a temperature-dependent functional form and coefficients used as tuning parameters for data fitting. Consequently, apparent equilibrium constants embed system non ideality and activity coefficients are set to unity due to the ideal solution assumption[13].

Several applications and modifications of the Kent-Eisenberg model are recorded in the literature. Among these, Jou et al.[46] limit the tuning parameters of the equilibrium constants to the protonation equations only, varying their functional equation with a dependence on temperature, alkanolamine concentration and pressure. Hu and Chakma[47,48] assume apparent equilibrium constant for AMP and DGA protonation to depend on liquid-phase gas concentration and alkanolamine concentration. Li and Shen[49] introduce a correction of the chemical equilibrium constants composed of a temperature-dependent factor multiplied by an activity-dependent-based constant, which is a function of loading, amine concentration and includes tuneable parameters. This last contribution has been debated in the literature[13] as the use of loading in activity coefficient-based equilibrium contribution affects the model's predictive capabilities.

To further simplify the iterative approach initially proposed by Kent and Eisenberg, a mathematical algorithm has been introduced by Haji-Sulaiman et al. in 1998[50] to solve the thermodynamic problem with a single polynomial equation as a function of hydrogen ion concentration. The selected root belongs to a pH interval of 7-11 and it can be used to determine speciation.

Successive KE modifications in the literature propose different apparent equilibrium constant expressions, which attempt to reproduce the composition dependency properly belonging to the activity coefficients formulation that is neglected by assumption[51]. This simple approach has been widely spread and adopted by the industry, however modelling results highlight that KE provides satisfactory performance for medium loadings only, presenting higher deviations in the low and high loading range. In addition to this, KE is not thermodynamically-sound, and it is intrinsically not predictive due to the lack of activity coefficients.

In the present investigation, a revised KE model is proposed and calibrated against a dataset constituted by VLE data at 33.1 $\%_{w/w}$ LysK concentration at absorber conditions[44] and VLE data at 33.5 $\%_{w/w}$ LysK concentration at stripper conditions[52]. This dataset has been selected as it covers a fair loading range (0.5 – 1.5 molCO_2/molLysK) compared to other experimental literature data, and a broad temperature window (298 K – 393 K). Moreover, the selected dataset shows reduced data dispersion (see supplementary material for further details on identified datasets).

KE adoption has been necessary to compensate missing equilibrium constants, i.e. carbamate hydrolysis and amino acid protonation from the set of equations Eq. 8 – Eq. 14. With respect to equilibrium constants referred to protonated AAS dissociation, experimental data from Nagai et al.[53] have been interpolated in a temperature range spanning from 283.1 K to 333.1 K. Consequently, coefficients for temperature-dependent equilibrium constant of carbamate hydrolysis reactions have been estimated by VLE data regression. Moreover, the edition of the KE correlation proposed for this study is endowed with an activity coefficient model based on Debye–Hückel formulation (Paragraph 2.4). Debye–Hückel limiting law describes non-ideal behaviour due to electrostatic forces in extremely dilute electrolyte solutions[54]. Therefore, while regressing the missing equilibrium constants, this revised KE version is expected to provide reasonable extrapolation of the vapour-liquid equilibria in a lower loading range, steering KE outside its calibration range.

In line with the recent literature on the topic, ideal gas phase has been assumed and CO_2 phase equilibrium has been described using Henry's law ($\widehat{\varphi}^{v}_{CO_2}$ and Poynting factor further discussed in the supplementary material are set to 1).

Within this framework, the revised KE is propaedeutic to the definition of a related Deshmukh-Mather model as **(i)** it requires the selection of a robust dataset for model calibration and **(ii)** the equilibrium constants (related to the two carbamate hydrolysis reactions) estimated within the KE framework can be embedded in the Deshmukh-Mather model.

Figure 2 reports a scheme of the adopted revised Kent-Eisenberg approach. The model has been implemented in Matlab® and the temperature-dependent coefficients of the apparent equilibrium constants minimise the selected objective function with Matlab® fminsearch function. The objective function F_{obj} minimised during the parameter regression is reported in Eq.19 and it accounts for the deviation between experimental and modelled CO_2 partial pressure. Results of the regression against experimental data are reported in Table 1, meanwhile identified equilibrium constants used to solve the thermodynamic problem are reported in Section 4.

$$F_{obj} = \sum_{i=1}^{n} \left(\frac{p_{CO_2,i}^{Exp} - p_{CO_2,i}^{Model}}{p_{CO_{2,\mathrm{i}}}^{Exp}} \right)^2 \qquad \textit{Eq. 19}$$

Table 1: Kent-Eisenberg correlation regression against Shen's VLE data set.

Equilibrium constants	Cf. Section 4	
Experimental dataset (Shen et al.[44] and Li et al.[52])	**N. experimental data**	97 [-]
	Temperature range	298-393 K
	Loading range	0.5 – 1.5 molCO_2/ molLysK
Tolerance	1.00E-04	[-]
Average absolute deviation – AAD%†	9	%

†AAD = $100 \frac{\sum_{i=1}^{n} \left| \frac{p_{CO_2,i}^{Exp} - p_{CO_2,i}^{Model}}{p_{CO_{2,\mathrm{i}}}^{Exp}} \right|}{n}$ [%]

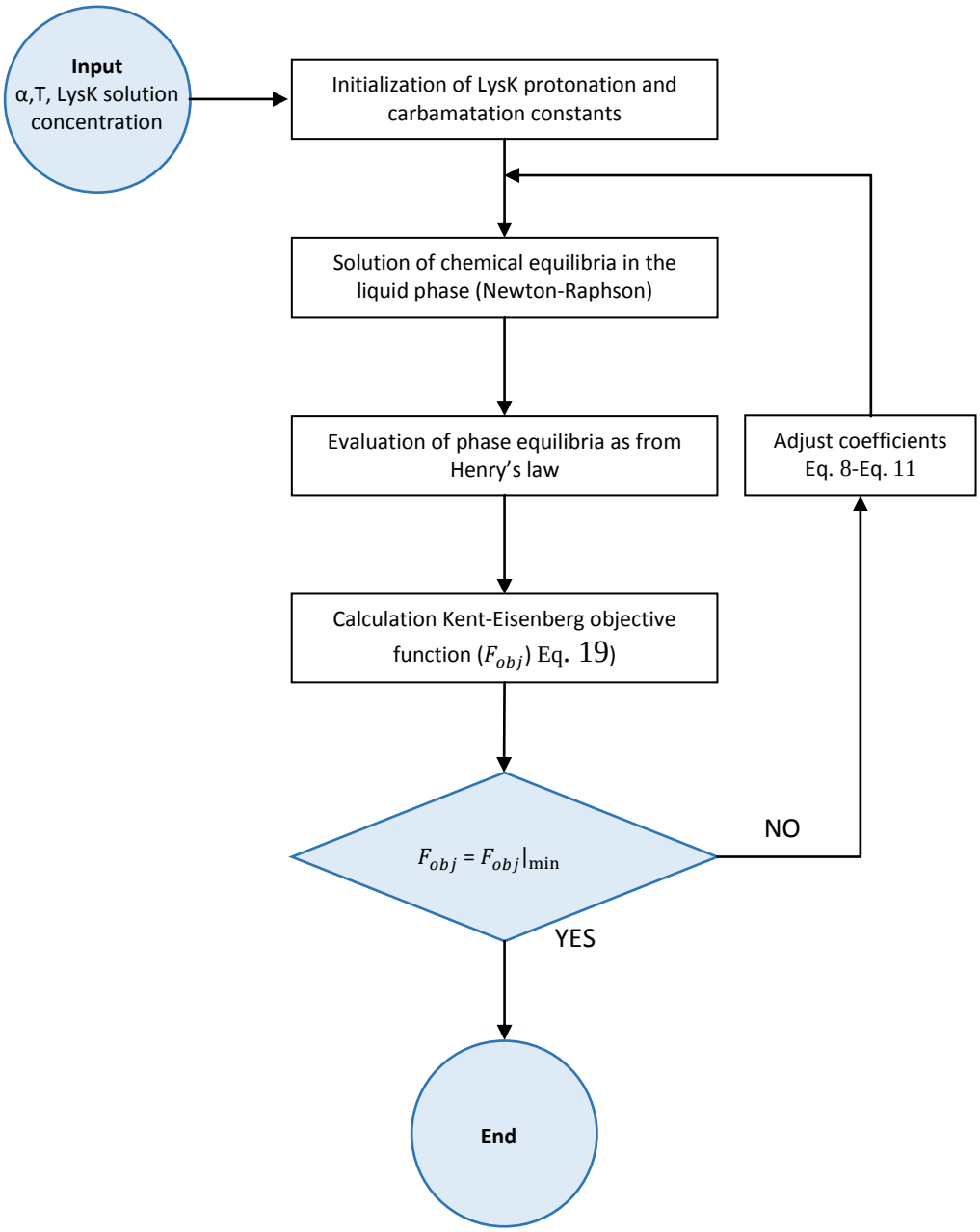

Figure 2: Revised Kent-Eisenberg algorithm.

2.4. Deshmukh-Mather Model

The Deshmukh-Mather model calculates the excess Gibbs free energy using the activity coefficient equation proposed by Guggenheim and Stokes[55], which is essentially an extension of the Debye-Hückel model. The corresponding activity coefficient equation (Eq. 20) consists in a first term expressing the Debye-Hückel law accounting for the electrostatic forces, and a second and correlative term which is added to consider short-range van der Waals interactions. The adjusted parameters in this model are the r_i length in the Debye-Hückel term (in Å; comparable to an ion radius), and the β_{ij} binary interaction coefficients (in kg H_2O/mol).

$$\ln \ddot{\gamma}_i = -\frac{A z_i^2 I^{1/2}}{1 + B r_i I^{1/2}} + 2 \sum_j \beta_{ij}\, m_j \qquad \textit{Eq. 20}$$

Where z_i is the component charge number, m_i its molality (mol/kg H_2O), and $I = \frac{1}{2}\sum_j z_j^2 m_j$ is the molality-scale ionic force (mol/kg H_2O).

Parameters used in the Deshmukh-Mather model can be found in the Supplementary Materials. A conventional formulation of the β_{ij} term from the Guggenheim equation is showed in Eq. 21.

$$\beta_{ij} = a_{ij} + b_{ij}\mathrm{T} \qquad \textit{Eq. 21}$$

The DM model developed to describe CO_2 solubility in LysK aqueous solutions is based on the following assumptions: **(i)** the model inherits the equilibrium constants coefficients provided by VLE data regression from KE; **(ii)** DM calibration has been carried out by tuning parameters a_{ij} and b_{ij} against the same VLE dataset used for KE.

The DM regression algorithm and objective functions are consistent with the ones reported in Figure 2 for KE. Results of the regression to identify binary interaction parameters β_{ij} are reported in Section 4. The solution scheme of the liquid-phase chemical reaction system and of the vapour-liquid equilibria is reported in Figure 3.

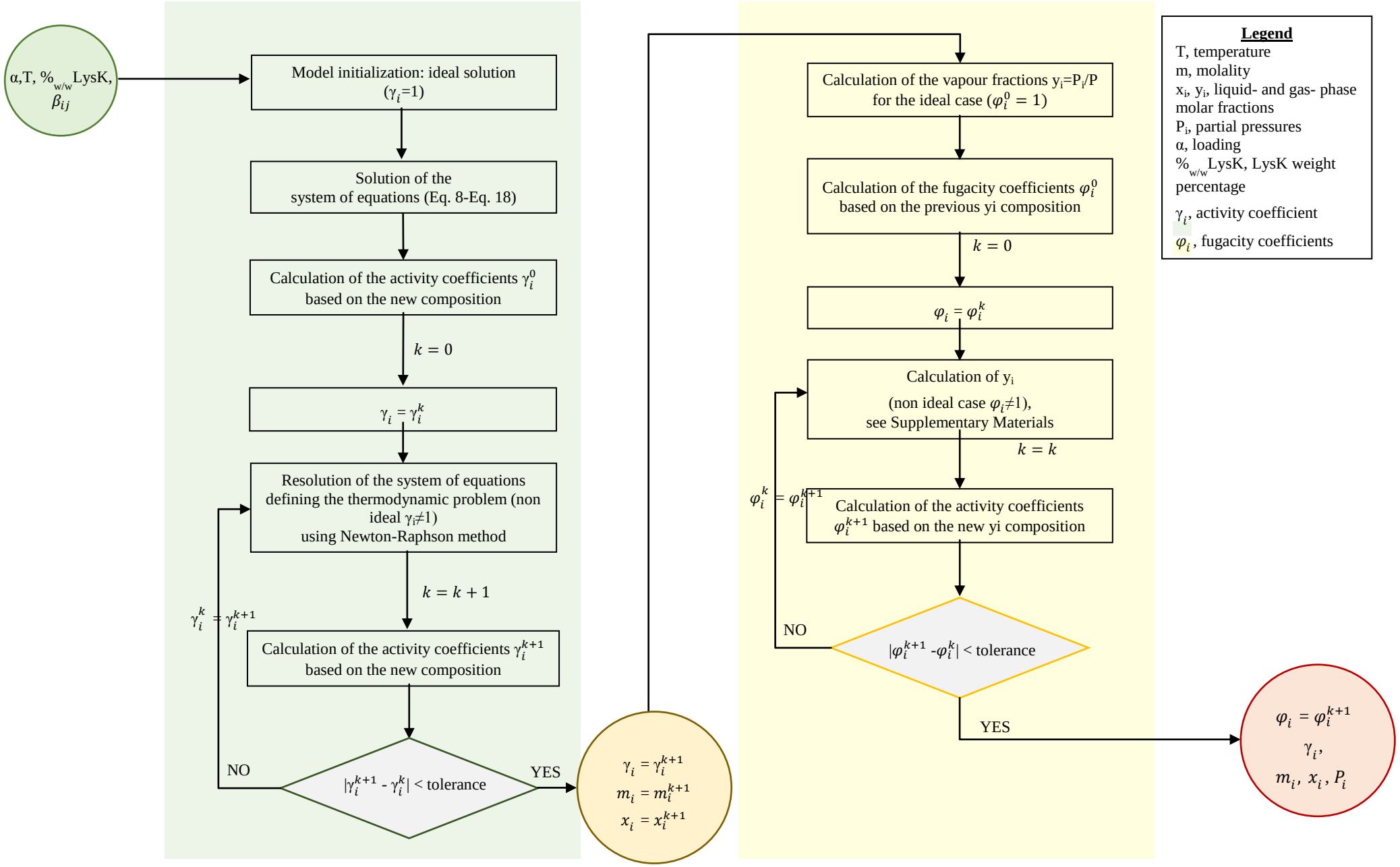

Figure 3: Main algorithm describing DM model.

3. Approach and Methodology

Within the present work, a thermodynamic model of CO_2 solubility in the alternative aqueous LysK solvent has been developed starting from an enhanced Kent-Eisenberg correlation calibrated for 33.1 and 33.5%$_{w/w}$ aqueous LysK VLE data from Shen et al.[44] and Li et al.[52]. Model calibration has been carried out selecting data among the highest available concentrations from the literature[44,52,56], as recommended in previous work assessing solvent capacity against a reference commercial solvent (i.e., 30%$_{w/w}$ MEA aqueous solution) at bench-scale[6,39] for NGCC-flue gas decarbonisation (i.e., ~4% CO_2 molar fraction in the flue gas). Moreover, the selected data set is characterized by consistent data in a wide loading and temperature range and it has been identified among a number of different literature sources[37,44,52,57–61].

KE modelling results are twofold: a complete set of constants representative of the investigated system is identified after regression against VLE data for LysK solutions at 33.1% $_{w/w}$ and 33.5%$_{w/w}$, loading between 0.5 - 1.5 molCO_2/molLysK and a temperature range of 298.1 – 393.1 K, representative of absorption and stripping conditions. Moreover, a novel KE formulation endowed with Debye-Hückel activity coefficients has been developed. Although based on regression, the set of equilibrium constants defined from KE-model can be embedded in a thermodynamically sound Deshmukh-Mather model describing CO_2 solubility in aqueous LysK solutions. Deshmukh-Mather parameter regression over the selected dataset has been carried out over the same data set used for KE regression, tuning β_{ij}terms. Species pairs to investigate have been selected as from Weiland et al.[62]: interactions between like-charged ions are discarded, as well as molecule self-interactions (excluding MEA) and interactions between water and its ionization products. Further, interactions between the acid gas and other components have been disregarded. Results of KE correlation, equilibrium constant parameters, Deshmukh-Mather model, and adjusted binary interaction parameters are described in Section 4. A visual summary of the methodology is showed in Figure 4.

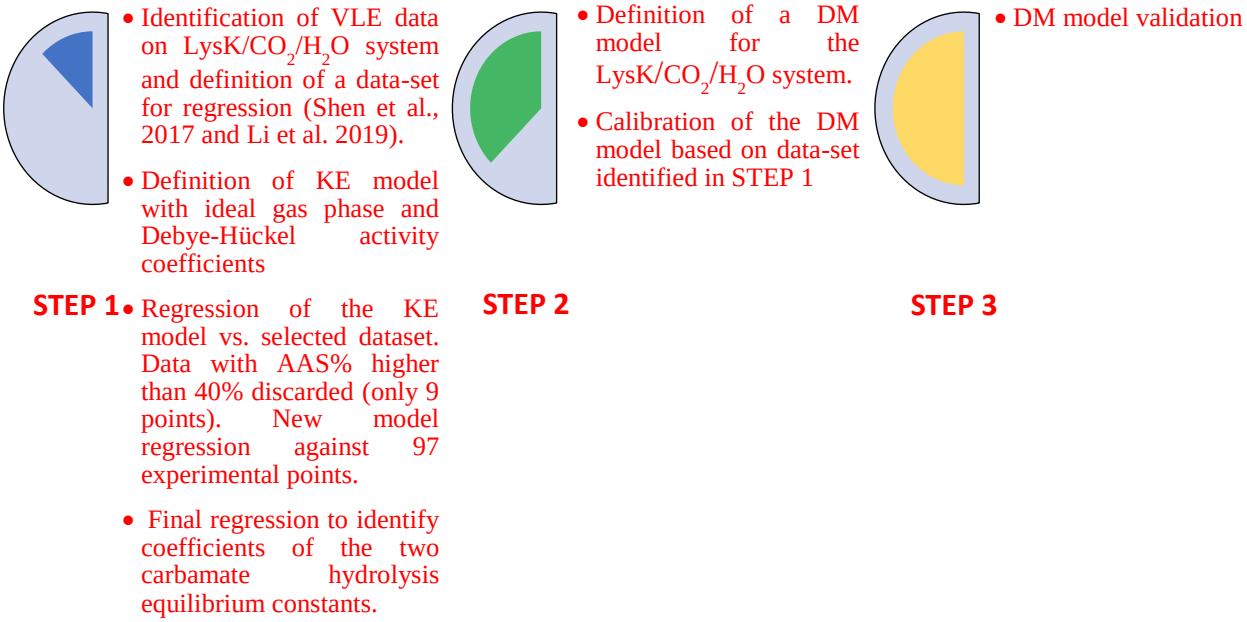

Figure 4: Main steps leading to the definition of a Deshmukh-Mather model for the LysK/CO_2/H_2O system.

4. Results and Discussion

While developing KE model, coefficients of carbamate hydrolysis reactions (K_{R1}, K_{R2}) have been adjusted over 33.1 and 33.5%$_{w/w}$ potassium lysinate-VLE data described in Section 3, setting CO_2 hydrolysis (K_{CO_2}), bicarbonate dissociation ($K_{HCO_3^-}$) and water dissociation (K_{H_2O}) coefficients from the literature. AAS dissociation constants have been identified by interpolating experimental data from Nagai et al.[53] in a temperature range spanning from 283.1 K to 333.1 K; this implies that the models (both KE and DM)

extrapolates values of the aforementioned equilibrium constants due to the high temperature range for calibration. Table 2 reports he complete set of coefficients and associated temperature range; information comes both from the literature – with references – and Kent-Eisenberg correlation developed in this work.

Table 2: Proposed equilibrium constants for the LysK/CO_2/H_2O system as a function of temperature (molal base).

Constant (Molality based)	**Functional form: $ln(K_i) = a + \frac{b}{T}$ + cln(T) + dT+$\frac{e}{T^2}$**						**Notes**
	a	**b**	**c**	**d**	**e**	**ΔT [°C]**	
K_{R1}	7.7594E-01	-8.0245E+02	0	0	0	25-120	Present work – regressed with revised KE
K_{R2}	1.2759E+01	-4.3795E+03	0	0	0	25-120	Present work – regressed with revised KE
K_{LysH^+}	-3.5851E+01	0	0	5.0100E-02	0	10-60	Data interpolated from Nagai et al.[53]
K_{LysH}	-1.2193E+02	0	1.7032E+01	0	0	10-60	Data interpolated from Nagai et al.[53]
K_{CO_2}	-1.2030E+03	6.8359E+04	1.8844E+02	-2.0642E-01	-4.7129E+06	0-400	[63]
$K_{HCO_3^-}$	1.7536E+02	-7.2306E+03	-3.0651E+01	1.3148E-02	-3.7281E+05	0-250	[63]
K_{H_2O}	1.409E+02	-1.3445E+04	-2.2477E+01	0	0	0-225	[63,64]

The revised Kent-Eisenberg model fits the experimental data from Shen et al. and Li et al. at 33.1 and 33.5 $\%_{w/w}$ aqueous LysK solution adequately (see Figure 5), showing better accuracy in the middle loading range. The model (AAD = 9%) embeds an activity coefficient correction from Debye–Hückel, which provides a more accurate theoretical foundation, steering extrapolation. The parity plot is reported in Figure 6, highlighting 15% error bar between model response and experimental data.

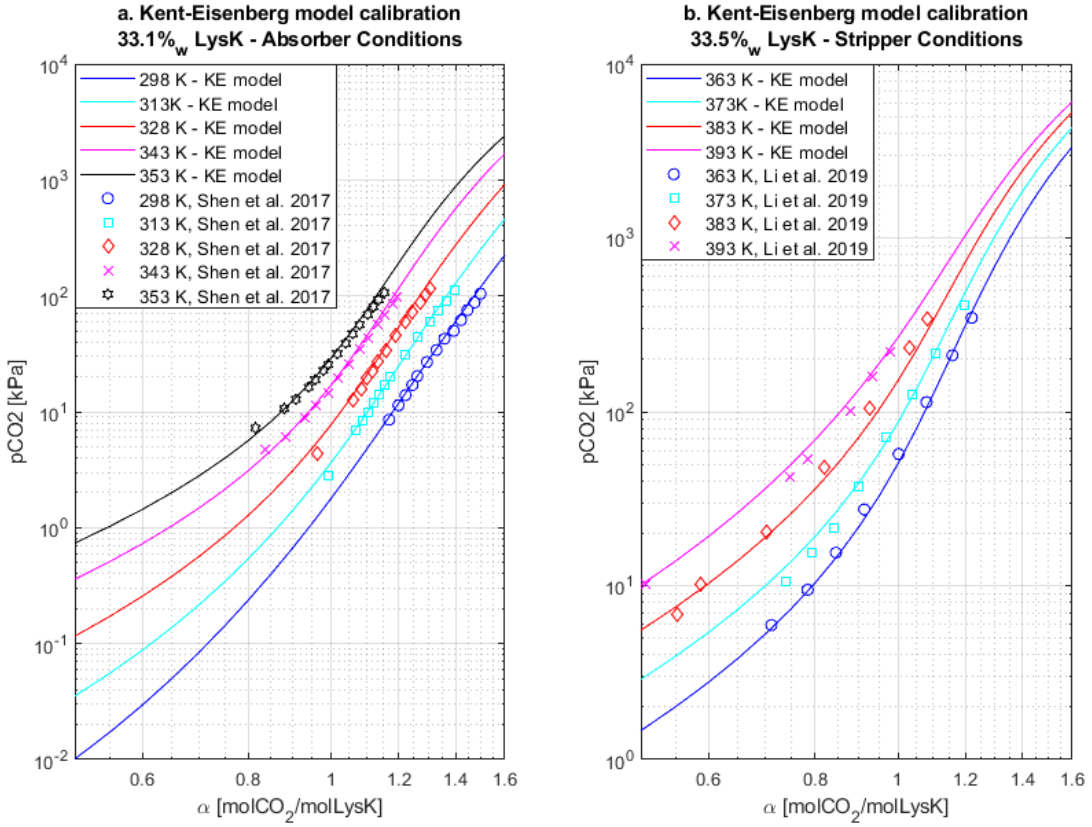

*Figure 5: Results of the revised KE model representing CO_2 solubility in **a.** 33.1%w/w and **b.** 33.5%w/w LysK aqueous solution.*

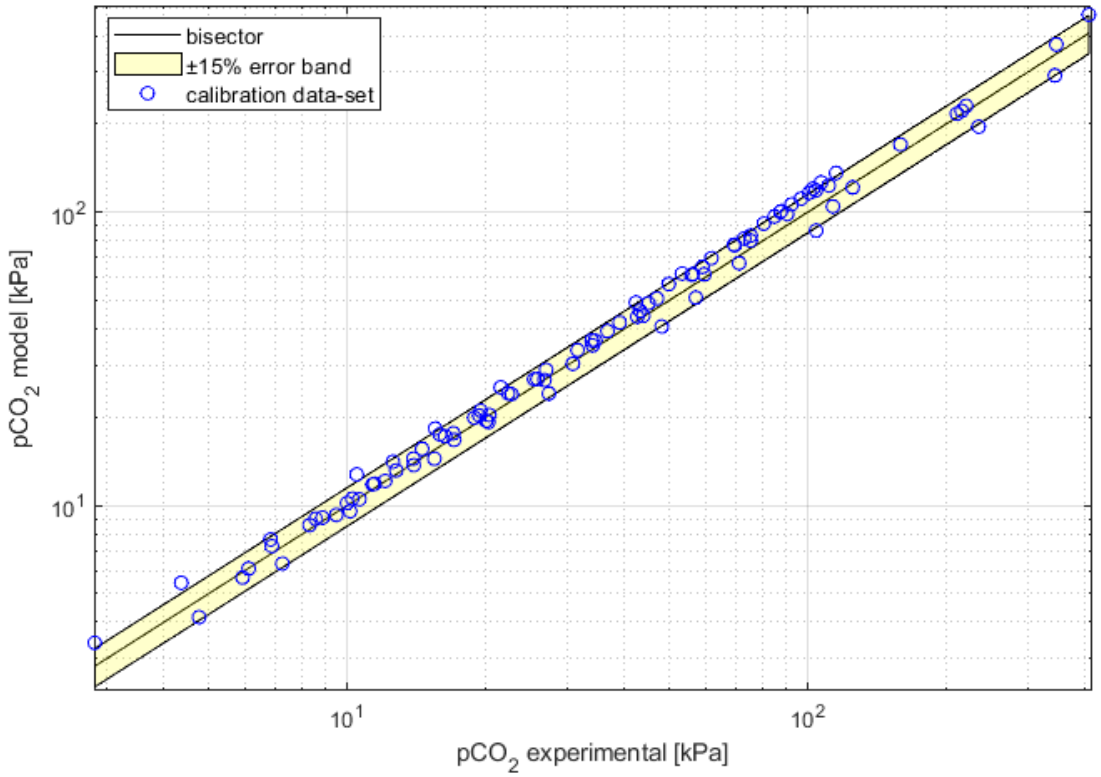

Figure 6: Parity plot representative of the results of the revised KE model for CO_2 solubility in 33.1 and 33.5%w/w LysK aqueous solution.

KE is an empirical correlation used for data fitting. Within this work, KE has paved the ground for the implementation of the Deshmukh-Mather model. Given the lack of complete CO_2 VLE data, extrapolation with KE is supported by the activity coefficients from Debye–Hückel, preserving physical significance in the solubility profiles (p_{CO2} vs. loading isotherms at different temperatures). From the analysis of the dataset, it stands out that future VLE experimental campaigns should measure CO_2 solubility in aqueous LysK over complete loading range (0.1-1.5 molCO_2/molLysK), allowing proper DM calibration.

Data fitting provided by the revised KE model is appropriate and most of the model results fall within a ±15% error bar (Figure 6). Despite the introduction of activity coefficients in the revised Kent-Eisenberg, the correlation remains an empirical model, developed to fill the literature gap, mainly consisting in the lack of selected equilibrium constants for the LysK/CO_2/H_2O system. To set the ground for further breakthroughs providing independently-measured and validated equilibrium constants, and working towards a valid and thermodynamically-sound model, a complete Deshmukh-Mather model is proposed in the present study. The model contains temperature-dependent parameters (e.g., Henry coefficient, equilibrium constants, Debye-Hückel term in the activity coefficient expression) and composition-dependent non-ideality is also included in the Guggenheim equation, which relies on both ionic strength and individual constituent molalities (Paragraph 2.4). DM model has been calibrated against the same dataset used for KE calibration, regressing binary interaction coefficients in Matlab® (fminsearch function, objective function from Eq. 19). Adjusted Ion-ion, ion-molecule and molecule-molecule interaction parameter values selected according to Weiland et al.[62] (see Section 3) are reported in Table 3.

Table 3: Species interactions and regressed binary interaction parameters.

INTERACTIONS	**a_{ij} [kgH_2O/kmol]**	**b_{ij} [kgH_2O/kmolK]**
$LysH^+/NH_3^+ - R_2R_1CH - NH_2$	3.8616e+00	-1.6345e-01
$LysH^+/NH_2 - R_2R_1CH - NH_2$	5.4588e-01	-1.1619e+00
$LysH^+/HCO_3^-$	1.7302e+00	-2.8313e-02
$LysH^+/ CO_3^{2-}$	2.8097e-01	-1.3054e+00

Lys^-/Lys^-	1.2424e+00	2.8589e-02
$Lys^-/NH_3^+ - R_2R_1CH - NH_2$	-1.1361e-01	-1.0827e-01
$Lys^-/NH_2 - R_2R_1CH - NH_2$	7.9814e-01	4.8883e-01
Lys^-/HCO_3^-	-1.5917e+00	-1.4828e+00

Figure 7 reports equilibrium isotherms of the DM model obtained after calibration (AAD = 7%), with related parity plot in Figure 8. Figure 9 shows speciation for a 33%w/w aqueous LysK system at 313.2 K. In Figure 10, DM model validation is represented.

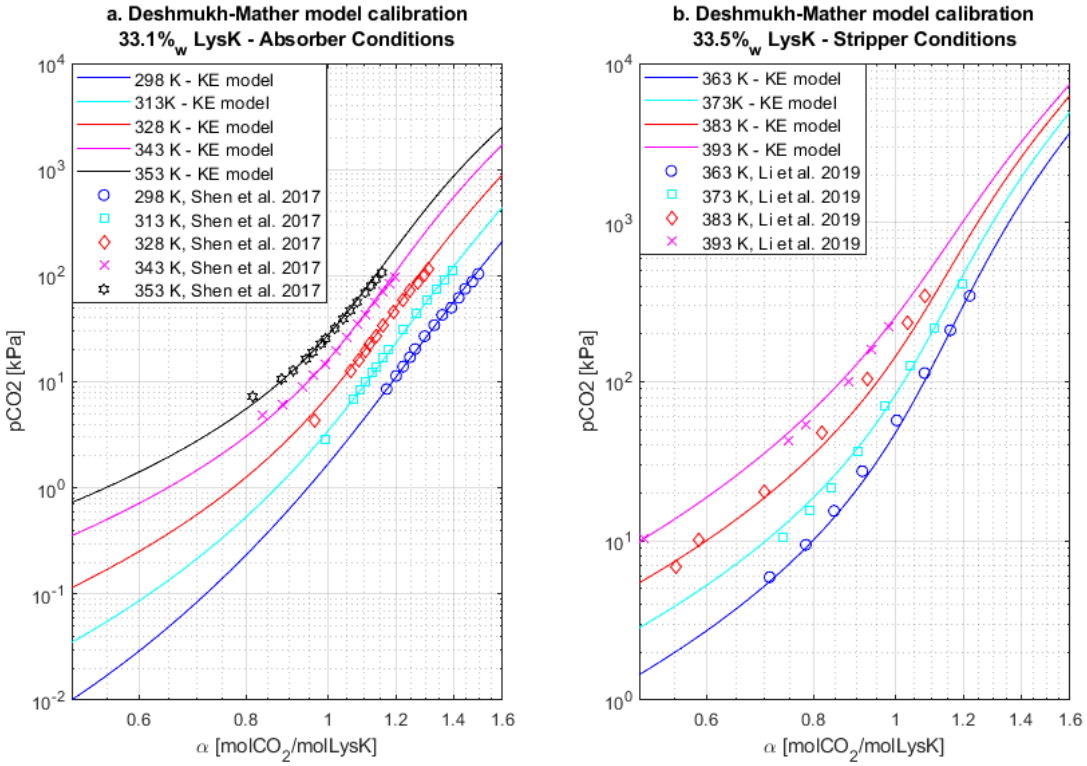

Figure 7: Deshmukh-Mather model representing CO_2 solubility in 33.1 and 33.5%$_{w/w}$ aqueous LysK solution.

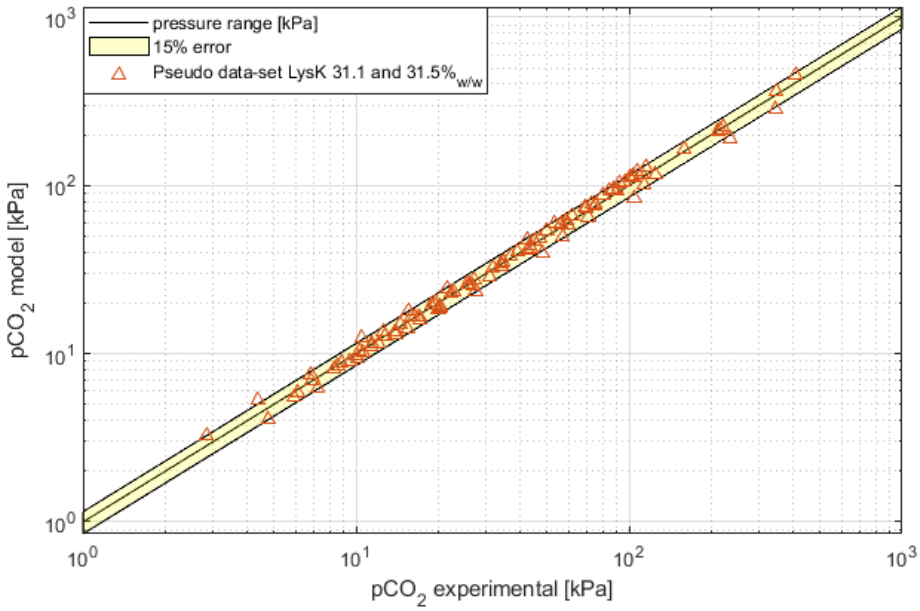

Figure 8: DM parity plot - CO_2 solubility in 33.1 and 33.5%w/w LysK aqueous solution.

.

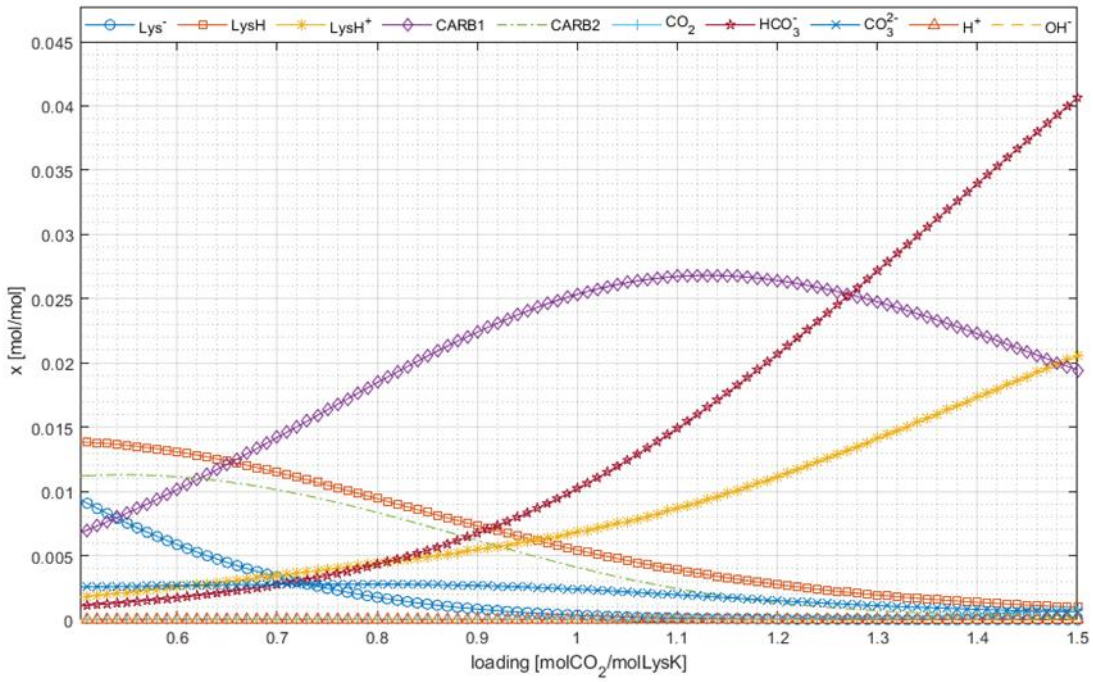

Figure 9: Speciation for 33.1%$_{w/w}$ aqueous LysK solution and 313.2K.

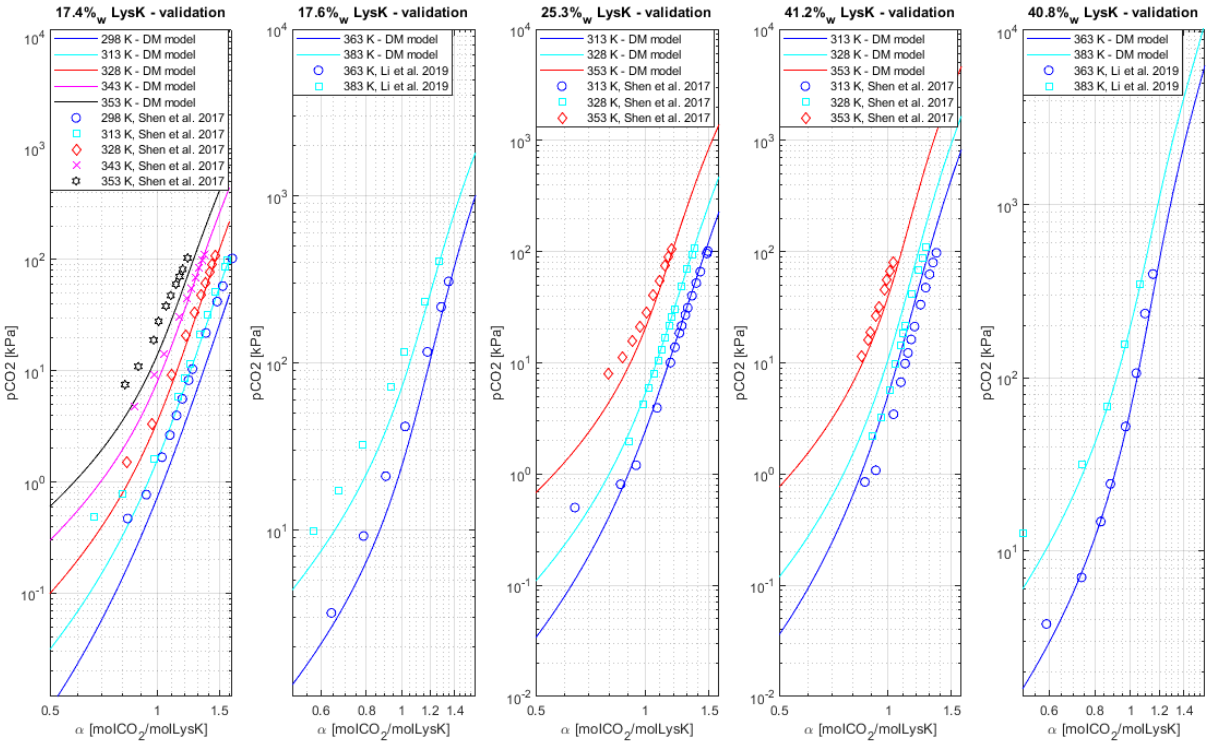

Figure 10: Solubility from DM model – validation for different selected solubility data.

Higher model deviation at low partial pressure can be attributed to the higher relative experimental error underlined by the data providers[44]: below 1 kPa, the recorded partial pressure of CO_2 is comparable with the maximum error provided by the pressure transducer (0.25 kPa) used during the test campaign. Moreover, the

overall standard uncertainty affecting the reported values of experimental CO_2 partial pressure is equal to 1.50 kPa[44], which significantly affects the accuracy of data at this order of magnitude (1 kPa). This also explains the scarcity of experimental data at such low partial pressures.

DM model properly fits the experimental data, showing slightly better accuracy than KE correlation (AAD - DM= 7%). An analysis of the Deshmukh-Mather outcome shows how the prediction accuracy is higher with respect to KE for medium-to-high CO_2 partial pressures. This trend is coherent with the addition of a short-range interaction term in the activity coefficient expression, which mainly rectifies the Henry's coefficient to account for non-ideality, with significant effects at high loadings.

5. Conclusions and perspectives

Potassium lysinate is being addressed as a solvent of interest in the field of post combustion capture of CO_2. The design of related absorption units operating with amino acid salts solutions is under investigation from both academia and industry. Absorption/stripping unit sizing and full process optimization require a reliable description of the thermodynamic system, developing accurate models to reproduce CO_2 solubility in LysK solutions.

A significant literature gap undermining the description of the LysK/CO_2/H_2O system exists because of the lack of carbamate hydrolysis equilibrium constants and in the limited data available for AAS protonation equilibrium constants. Moreover, limited loading range investigated in vapour-liquid equilibrium experiments for model regression, validation, and CO_2 solubility description in the selected solution as well as concerns on VLE data consistency can be highlighted after literature analysis.

The present work tackles the limits of the current state-of-the-art, implementing: **(i)** a revised Kent-Eisenberg correlation defined and endowed with Debye-Hückel activity coefficient model. The Kent-Eisenberg approach provides a set of equilibrium constant coefficients calculated via experimental data regression, and the Debye-Hückel activity coefficient model allows possible extrapolation of CO_2 solubility below the experimental loading range; **(ii)** starting from the equilibrium constant functions and identified VLE calibration dataset (p_{CO2} vs. loading) defined in point (i), a semi-empirical and thermodynamically-sound Deshmukh-Mather model has been defined and regressed against VLE data in the temperature range of 298.2-393.0 K already used for KE calibration. The activity coefficient model of Deshmukh-Mather is based on the Guggenheim equation.

Kent-Eisenberg and Deshmukh-Mather have been calibrated over data at 33.1%$_{w/w}$ 33.5% $_{w/w}$ aqueous LysK concentrations. CO_2 partial pressure prediction results in an average absolute deviation equal to 9% and 7% respectively, with reference to the experimental data used for calibration. Deshmukh-Mather relies on equilibrium constants provided by Kent-Eisenberg with a computational approach consisting in VLE data regression. However, it constitutes a first rigorous, semi-empirical model which can be improved upon availability of further experimental data. Moreover, DM theoretical foundations support its adoption beyond the calibration window.

Within this framework, future work should focus on expanding the available experimental VLE data to describe CO_2 solubility in a wide loading envelope. Equilibrium constants for carbamate hydrolysis reactions should be estimated based on measurements of e.g., NRM speciation. Also, additional experimental data should be provided to characterize equilibria for AAS protonation in a wider temperature range. The new experimental information both in terms of equilibrium constants and solubility should be used together with the currently available datasets to recalibrate and validate the Deshmukh-Mather model, avoiding the use of Kent-Eisenberg as a first step to complete the set of equilibrium constant. Lastly, modelling results should be compared against other widely adopted models such as e-NRTL.

ACKNOWLEDGEMENT

Author Antonio Conversano is grateful to Laboratorio Energia e Ambiente Piacenza - LEAP s.c.a r.l. for its support during the research work.

List of symbols

A	limit slope of Debye–Hückel
a	activity
Ds	solvent dielectric constant
f	fugacity (MPa)
F	Faraday constant (=eNA) (Cmol−1)
H	Henry constant (Pa kg of water mol−1)
K	equilibrium constant
I	ionic force
LysK	potassium lysinate
m	molality (mol kg−1 of water)
P	total pressure (Pa)
r	ionic radius (Å)
R	the gas constant (JK−1 mol−1)
T	temperature (K)
T_R	reduced temperature (T/T_C)
ν	partial molar volume (cm3 mol−1)
x	molar fraction in the liquid phase
y	molar fraction in the vapor phase
z	charge (C)
Z	compressibility factor

Greek letters

α	loading (molCO_2/molLysK)
βij	interaction parameter
ε_0	vacuum permittivity
φ	fugacity coefficient
a	activity coefficient
ω	acentric factor

Superscripts, subscripts, notation

exp	experimental
i,j	component
l	liquid phase
model	model result
obj	objective
v	vapour phase
¨	molal base
^	mixture
∞	infinite dilution

BIBLIOGRAPHY

(1) IEA. *Global Energy & CO2 Status Report*; 2019.

(2) IEA. *Energy Technology Perspectives 2020*; 2020.

(3) Wang, M.; Lawal, A.; Stephenson, P.; Sidders, J.; Ramshaw, C. Post-Combustion CO2 Capture with Chemical Absorption: A State-of-the-Art Review. *Chem. Eng. Res. Des.* **2011**, *89* (9), 1609–1624. https://doi.org/10.1016/j.cherd.2010.11.005.

(4) van Os, P. *CESAR-CO2 Enhanced Separation and Recovery*; 2006; Vol. 4.

(5) CaESAR. *European Best Practice Guidelines for Assessment of CO2 Capture Technologies*; 2011.

(6) Cremona, R.; Delgado, S.; Valtz, A.; Conversano, A.; Gatti, M.; Coquelet, C. Density and Viscosity Measurements and Modeling of CO 2 -Loaded and Unloaded Aqueous Solutions of Potassium Lysinate. *J. Chem. Eng. Data* **2021**, *66* (12), 4460–4475. https://doi.org/10.1021/acs.jced.1c00520.

(7) Budzianowski, W. M. *Energy Efficient Solvents for CO2 Capture by Gas-Liquid Absorption*; Budzianowski, W. M., Ed.; Green Energy and Technology; Springer International Publishing: Cham, 2017. https://doi.org/10.1007/978-3-319-47262-1.
(8) Sang Sefidi, V.; Luis, P. Advanced Amino Acid-Based Technologies for CO 2 Capture: A Review. *Ind. Eng. Chem. Res.* **2019**, *58* (44), 20181–20194. https://doi.org/10.1021/acs.iecr.9b01793.
(9) Jockenhövel, T.; Schneider, R. Towards Commercial Application of a Second-Generation Post-Combustion Capture Technology — Pilot Plant Validation of the Siemens Capture Process and Implementation of a First Demonstration Case. *Energy Procedia* **2011**, *4*, 1451–1458. https://doi.org/10.1016/j.egypro.2011.02.011.
(10) Conversano, A. *Thermodynamic Modelling and Process Design of a CO2 Capture Unit with Amino Acid Salts Solutions for Combined Cycle Decarbonisation*; Politecnico di Milano - PhD Thesis, 2021.
(11) Conversano, A.; Porcu, A.; Mureddu, M.; Pettinau, A.; Gatti, M. Bench-Scale Experimental Tests and Data Analysis on CO2 Capture with Potassium Prolinate Solutions for Combined Cycle Decarbonization. *Int. J. Greenh. Gas Control* **2020**, *93*, 102881. https://doi.org/10.1016/j.ijggc.2019.102881.
(12) Majchrowicz, M. E.; Brilman, D. W. F. Solubility of CO2 in Aqueous Potassium L-Prolinate Solutions—Absorber Conditions. *Chem. Eng. Sci.* **2012**, *72*, 35–44. https://doi.org/https://doi.org/10.1016/j.ces.2011.12.014.
(13) Suleman, H.; Maulud, A. S.; Man, Z. Review and Selection Criteria of Classical Thermodynamic Models for Acid Gas Absorption in Aqueous Alkanolamines. *Rev. Chem. Eng.* **2015**, *31* (6). https://doi.org/10.1515/revce-2015-0030.
(14) Mondal, B. K.; Bandyopadhyay, S. S.; Samanta, A. N. VLE of CO2 in Aqueous Sodium Glycinate Solution – New Data and Modeling Using Kent–Eisenberg Model. *Int. J. Greenh. Gas Control* **2015**, *36*, 153–160. https://doi.org/10.1016/j.ijggc.2015.02.010.
(15) Aftab, A.; M. Shariff, A.; Garg, S.; Lal, B.; Shaikh, M. S.; Faiqa, N. Solubility of CO2 in Aqueous Sodium β-Alaninate: Experimental Study and Modeling Using Kent Eisenberg Model. *Chem. Eng. Res. Des.* **2018**, *131*, 385–392. https://doi.org/10.1016/j.cherd.2017.10.023.
(16) Garg, S.; Shariff, A. M.; Shaikh, M. S.; Lal, B.; Aftab, A.; Faiqa, N. VLE of CO 2 in Aqueous Potassium Salt of L-Phenylalanine: Experimental Data and Modeling Using Modified Kent-Eisenberg Model. *J. Nat. Gas Sci. Eng.* **2016**, *34*, 864–872. https://doi.org/10.1016/j.jngse.2016.07.047.
(17) Syalsabila, A.; Maulud, A. S.; Suleman, H.; Hadi Md Nordin, N. A. VLE of Carbon Dioxide-Loaded Aqueous Potassium Salt of L -Histidine Solutions as a Green Solvent for Carbon Dioxide Capture: Experimental Data and Modelling. *Int. J. Chem. Eng.* **2019**, *2019*, 1–11. https://doi.org/10.1155/2019/9428638.
(18) Chang, Y.-T.; Leron, R. B.; Li, M.-H. Carbon Dioxide Solubility in Aqueous Potassium Salt Solutions of L-Proline and Dl-α-Aminobutyric Acid at High Pressures. *J. Chem. Thermodyn.* **2015**, *83*, 110–116. https://doi.org/10.1016/j.jct.2014.12.010.
(19) Chen, C.-C.; Evans, L. B. A Local Composition Model for the Excess Gibbs Energy of Aqueous Electrolyte Systems. *AIChE J.* **1986**, *32* (3), 444–454. https://doi.org/10.1002/aic.690320311.
(20) Deshmukh, R. D.; Mather, A. E. A Mathematical Model for Equilibrium Solubility of Hydrogen Sulfide and Carbon Dioxide in Aqueous Alkanolamine Solutions. *Chem. Eng. Sci.* **1981**, *36* (2), 355–362. https://doi.org/10.1016/0009-2509(81)85015-4.
(21) Moioli, S.; Ho, M. T.; Wiley, D. E.; Pellegrini, L. A. Thermodynamic Modeling of the System of CO2 and Potassium Taurate Solution for Simulation of the Carbon Dioxide Capture Process. *Chem. Eng. Res. Des.* **2018**, *136*, 834–845. https://doi.org/10.1016/j.cherd.2018.06.032.
(22) Orlov, A. A.; Valtz, A.; Coquelet, C.; Rozanska, X.; Wimmer, E.; Marcou, G.; Horvath, D.; Poulain, B.; Varnek, A.; de Meyer, F. Computational Screening Methodology Identifies Effective Solvents for CO2 Capture. *Commun. Chem.* **2022**, *5* (1), 37. https://doi.org/10.1038/s42004-022-00654-y.
(23) Suleman, H.; Maulud, A. S.; Fosbøl, P. L.; Nasir, Q.; Nasir, R.; Shahid, M. Z.; Nawaz, M.; Abunowara, M. A Review of Semi-Empirical Equilibrium Models for CO2-Alkanolamine-H2O Solutions and Their Mixtures at High Pressure. *J. Environ. Chem. Eng.* **2021**, *9* (1), 104713. https://doi.org/10.1016/j.jece.2020.104713.
(24) Renon, H.; Prausnitz, J. M. Local Compositions in Thermodynamic Excess Functions for Liquid Mixtures. *AIChE J.* **1968**, *14* (1), 135–144. https://doi.org/10.1002/aic.690140124.
(25) Pitzer, K. S. Electrolytes. From Dilute Solutions to Fused Salts. *J. Am. Chem. Soc.* **1980**, *102* (9), 2902–2906. https://doi.org/10.1021/ja00529a006.

(26) Gregor, H. P. Electrolyte Solutions. R. A. Robinson and R. H. Stokes. Academic Press, New York, 1959. Xv + 559 Pp. $11.50. *J. Appl. Polym. Sci.* **1960**, *3* (8), 255–255. https://doi.org/10.1002/app.1960.070030823.
(27) Austgen, D. M.; Rochelle, G. T.; Peng, X.; Chen, C. C. Model of Vapor-Liquid Equilibria for Aqueous Acid Gas-Alkanolamine Systems Using the Electrolyte-NRTL Equation. *Ind. Eng. Chem. Res.* **1989**, *28* (7), 1060–1073. https://doi.org/10.1021/ie00091a028.
(28) N. Borhani, T.; Nabavi, S. A.; Hanak, D. P.; Manovic, V. Thermodynamic Models Applied to CO 2 Absorption Modelling. *Rev. Chem. Eng.* **2020**. https://doi.org/10.1515/revce-2019-0058.
(29) Plaza, J. M.; Wagener, D. Van; Rochelle, G. T. Modeling CO2 Capture with Aqueous Monoethanolamine. *Energy Procedia* **2009**, *1* (1), 1171–1178. https://doi.org/10.1016/j.egypro.2009.01.154.
(30) Thomsen, K.; C. Iliuta, M.; Rasmussen, P. Extended UNIQUAC Model for Correlation and Prediction of Vapor–Liquid–Liquid–Solid Equilibria in Aqueous Salt Systems Containing Non-Electrolytes. Part B. Alcohol (Ethanol, Propanols, Butanols)–Water–Salt Systems. *Chem. Eng. Sci.* **2004**, *59* (17), 3631–3647. https://doi.org/10.1016/j.ces.2004.05.024.
(31) Aronu, U. E.; Gondal, S.; Hessen, E. T.; Haug-warberg, T.; Hartono, A.; Hoff, K. A.; Svendsen, H. F. Solubility of CO 2 in 15 , 30 , 45 and 60 Mass % MEA from 40 to 120 1 C and Model Representation Using the Extended UNIQUAC Framework. *Chem. Eng. Sci.* **2011**, *66* (24), 6393–6406. https://doi.org/10.1016/j.ces.2011.08.042.
(32) Faramarzi, L.; Kontogeorgis, G. M.; Thomsen, K.; Stenby, E. H. Thermodynamic Modeling of the Solubility of CO2 in Aqueous Alkanolamine Solutions Using the Extended UNIQUAC Model Application to Monoethanolamine and Methyldiethanolamine. *Energy Procedia* **2009**, *1* (1), 861–867. https://doi.org/10.1016/j.egypro.2009.01.114.
(33) Fredenslund, A.; Jones, R. L.; Prausnitz, J. M. Group-Contribution Estimation of Activity Coefficients in Nonideal Liquid Mixtures. *AIChE J.* **1975**, *21* (6), 1086–1099. https://doi.org/10.1002/aic.690210607.
(34) Ye, K.; Freund, H.; Sundmacher, K. Modelling (Vapour+liquid) and (Vapour+liquid+liquid) Equilibria of {water (H2O)+methanol (MeOH)+dimethyl Ether (DME)+carbon Dioxide (CO2)} Quaternary System Using the Peng–Robinson EoS with Wong–Sandler Mixing Rule. *J. Chem. Thermodyn.* **2011**, *43* (12), 2002–2014. https://doi.org/10.1016/j.jct.2011.07.016.
(35) Pahlavanzadeh, H.; Nourani, S.; Saber, M. Experimental Analysis and Modeling of CO2 Solubility in AMP (2-Amino-2-Methyl-1-Propanol) at Low CO2 Partial Pressure Using the Models of Deshmukh–Mather and the Artificial Neural Network. *J. Chem. Thermodyn.* **2011**, *43* (12), 1775–1783. https://doi.org/10.1016/j.jct.2011.05.032.
(36) Mai Lerche, B. *CO 2 Capture from Flue Gas Using Amino Acid Salt Solutions*; 2012.
(37) Shen, S.; Yang, Y.; Wang, Y.; Ren, S.; Han, J.; Chen, A. CO2 Absorption into Aqueous Potassium Salts of Lysine and Proline: Density, Viscosity and Solubility of CO2. *Fluid Phase Equilib.* **2015**, *399*, 40–49. https://doi.org/10.1016/j.fluid.2015.04.021.
(38) Shen, S.; Yang, Y.; Bian, Y.; Zhao, Y. Kinetics of CO 2 Absorption into Aqueous Basic Amino Acid Salt: Potassium Salt of Lysine Solution. *Environ. Sci. Technol.* **2016**, *50* (4), 2054–2063. https://doi.org/10.1021/acs.est.5b04515.
(39) Conversano, A.; Porcu, A.; Mureddu, M.; Pettinau, A.; Gatti, M. Bench-Scale Absorption Testing of Aqueous Potassium Lysinate as a New Solvent for CO2 Capture in Natural Gas-Fired Power Plants. *Int. J. Greenh. Gas Control* **2021**, *106*, 103268. https://doi.org/10.1016/j.ijggc.2021.103268.
(40) Nelson, D. L. (David L.; Cox, M. M. *Lehninger Principles of Biochemistry*; Fourth edition. New York : W.H. Freeman, 2005., 2005.
(41) Guo, C.; Holland, G. P. Investigating Lysine Adsorption on Fumed Silica Nanoparticles. *J. Phys. Chem. C* **2014**, *118* (44), 25792–25801. https://doi.org/10.1021/jp508627h.
(42) Kitadai, N.; Yokoyama, T.; Nakashima, S. ATR-IR Spectroscopic Study of L-Lysine Adsorption on Amorphous Silica. *J. Colloid Interface Sci.* **2009**, *329* (1), 31–37. https://doi.org/10.1016/j.jcis.2008.09.072.
(43) Nolting, D.; Aziz, E. F.; Ottosson, N.; Faubel, M.; Hertel, I. V.; Winter, B. PH-Induced Protonation of Lysine in Aqueous Solution Causes Chemical Shifts in X-Ray Photoelectron Spectroscopy. *J. Am. Chem. Soc.* **2007**, *129* (45), 14068–14073. https://doi.org/10.1021/ja072971l.
(44) Shen, S.; Zhao, Y.; Bian, Y.; Wang, Y.; Guo, H.; Li, H. CO2 Absorption Using Aqueous Potassium Lysinate Solutions: Vapor – Liquid Equilibrium Data and Modelling. *J. Chem. Thermodyn.* **2017**,

115, 209–220. https://doi.org/10.1016/j.jct.2017.07.041.
(45) Kent, R. L.; Elsenberg, B. BETTER DATA FOR AMINE TREATING. *Hydrocarbon Processing*. 1976, pp 87–90.
(46) Jou, F. Y.; Mather, A. E.; Otto, F. D. Solubility of Hydrogen Sulfide and Carbon Dioxide in Aqueous Methyldiethanolamine Solutions. *Ind. Eng. Chem. Process Des. Dev.* **1982**, *21* (4), 539–544. https://doi.org/10.1021/i200019a001.
(47) Hu, W.; Chakma, A. Modelling of Equilibrium Solubility of CO2 and H2S in Aqueous Amino Methyl Propanol (AMP) Solutions. *Chem. Eng. Commun.* **1990**, *94* (1), 53–61. https://doi.org/10.1080/00986449008911455.
(48) Hu, W.; Chakma, A. Modelling of Equilibrium Solubility of CO 2 and H 2 S in Aqueous Diglycolamine (DGA) Solutions. *Can. J. Chem. Eng.* **1990**, *68* (3), 523–525. https://doi.org/10.1002/cjce.5450680327.
(49) Li, M.-H.; Shen, K.-P. Calculation of Equilibrium Solubility of Carbon Dioxide in Aqueous Mixtures of Monoethanolamine with Methyldiethanolamine. *Fluid Phase Equilib.* **1993**, *85*, 129–140. https://doi.org/10.1016/0378-3812(93)80008-B.
(50) Haji-Sulaiman, M. Z.; Aroua, M. K.; Benamor, A. Analysis of Equilibrium Data of CO2 in Aqueous Solutions of Diethanolamine (DEA), Methyldiethanolamine (MDEA) and Their Mixtures Using the Modified Kent Eisenberg Model. *Chem. Eng. Res. Des.* **1998**, *76* (8), 961–968. https://doi.org/10.1205/026387698525603.
(51) Chakma, A.; Meisen, A. Improved Kent-Eisenberg Model for Predicting CO2 Solubilities in Aqueous Diethanolamine (DEA) Solutions. *Gas Sep. Purif.* **1990**, *4* (1), 37–40. https://doi.org/10.1016/0950-4214(90)80025-G.
(52) Li, C.; Zhao, Y.; Shen, S. Aqueous Potassium Lysinate for CO2 Capture: Evaluating at Desorber Conditions. *Energy & Fuels* **2019**, *33* (10), 10090–10098. https://doi.org/10.1021/acs.energyfuels.9b02659.
(53) Nagai, H.; Kuwabara, K.; Carta, G. Temperature Dependence of the Dissociation Constants of Several Amino Acids. *J. Chem. Eng. Data* **2008**, *53* (3), 619–627. https://doi.org/10.1021/je700067a.
(54) Thomsen, K. Aqueous Electrolytes Model Parameters and Process Simulation, 1997. https://doi.org/10.11581/dtu.
(55) Guggenheim, E. A.; Stokes, R. H. Activity Coefficients of 2 : 1 and 1 : 2 Electrolytes in Aqueous Solution from Isopiestic Data. *Trans. Faraday Soc.* **1958**, *54*, 1646. https://doi.org/10.1039/tf9585401646.
(56) Suleman, H.; Maulud, A. S.; Syalsabila, A. Thermodynamic Modelling of Carbon Dioxide Solubility in Aqueous Amino Acid Salt Solutions and Their Blends with Alkanolamines. *J. CO2 Util.* **2018**, *26*, 336–349. https://doi.org/10.1016/j.jcou.2018.05.014.
(57) Zhao, Y.; Shen, S.; Bian, Y.; Yang, Y. nan; Ghosh, U. CO2 Solubility in Aqueous Potassium Lysinate Solutions at Absorber Conditions. *J. Chem. Thermodyn.* **2017**, *111*, 100–105. https://doi.org/10.1016/j.jct.2017.03.024.
(58) Suleman, H.; Fosbøl, P. L. Physicochemical Data of Carbonic-Anhydrase-Blended Aqueous Potassium Lysinate Solutions as New Absorbents. *J. Chem. Eng. Data* **2020**, *65* (5), 2383–2391. https://doi.org/10.1021/acs.jced.9b00963.
(59) Zhao, Y.; Bian, Y.; Li, H.; Guo, H.; Shen, S.; Han, J.; Guo, D. A Comparative Study of Aqueous Potassium Lysinate and Aqueous Monoethanolamine for Postcombustion CO 2 Capture. *Energy & Fuels* **2017**, *31* (12), 14033–14044. https://doi.org/10.1021/acs.energyfuels.7b02800.
(60) Suleman, H.; Maulud, A. S.; Man, Z. Carbon Dioxide Solubility in Aqueous Potassium Lysinate Solutions: High Pressure Data and Thermodynamic Modeling. *Procedia Eng.* **2016**, *148*, 1303–1311. https://doi.org/10.1016/j.proeng.2016.06.543.
(61) Mazinani, S.; Ramazani, R.; Samsami, A.; Jahanmiri, A.; Van der Bruggen, B.; Darvishmanesh, S. Equilibrium Solubility, Density, Viscosity and Corrosion Rate of Carbon Dioxide in Potassium Lysinate Solution. *Fluid Phase Equilib.* **2015**, *396*, 28–34. https://doi.org/10.1016/j.fluid.2015.03.031.
(62) Weiland, R. H.; Chakravarty, T.; Mather, A. E. Solubility of Carbon Dioxide and Hydrogen Sulfide in Aqueous Alkanolamines. *Ind. Eng. Chem. Res.* **1993**, *32* (7), 1419–1430. https://doi.org/10.1021/ie00019a016.
(63) Kamps, Á. P.-S.; Balaban, A.; Jödecke, M.; Kuranov, G.; Smirnova, N. A.; Maurer, G. Solubility of Single Gases Carbon Dioxide and Hydrogen Sulfide in Aqueous Solutions of N -

Methyldiethanolamine at Temperatures from 313 to 393 K and Pressures up to 7.6 MPa: New Experimental Data and Model Extension. *Ind. Eng. Chem. Res.* **2001**, *40* (2), 696–706. https://doi.org/10.1021/ie000441r.

(64) Jakobsen, J. P.; Krane, J.; Svendsen, H. F. Liquid-Phase Composition Determination in CO2−H2O−Alkanolamine Systems: An NMR Study. *Ind. Eng. Chem. Res.* **2005**, *44* (26), 9894–9903. https://doi.org/10.1021/ie048813+.